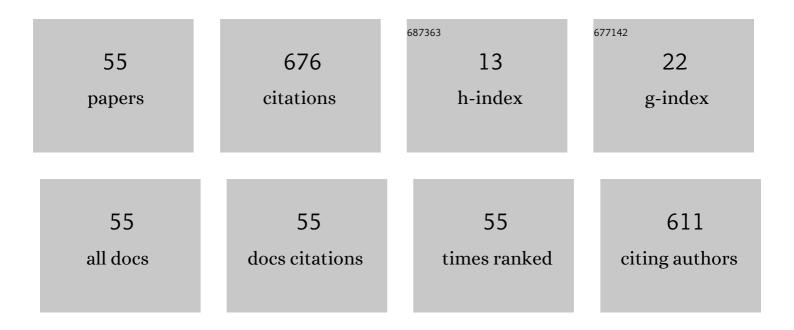
Rabaah Syahidah binti Azis

List of Publications by Year in descending order

Source: https://exaly.com/author-pdf/641699/publications.pdf Version: 2024-02-01



#	Article	IF	CITATIONS
1	Structural and magnetic properties of yttrium iron garnet (YIG) and yttrium aluminum iron garnet (YAIG) nanoferrite via sol-gel synthesis. Results in Physics, 2017, 7, 1135-1142.	4.1	79
2	Sintering behavior, ac conductivity and dielectric relaxation of Li 1.3 Ti 1.7 Al 0.3 (PO 4) 3 NASICON compound. Results in Physics, 2016, 6, 719-725.	4.1	51
3	Recent Advances in the Rejection of Endocrine-Disrupting Compounds from Water Using Membrane and Membrane Bioreactor Technologies: A Review. Polymers, 2021, 13, 392.	4.5	38
4	An investigation of microstructural, magnetic and microwave absorption properties of multi-walled carbon nanotubes/Ni0.5Zn0.5Fe2O4. Scientific Reports, 2019, 9, 15523.	3.3	29
5	Adsorptive Removal of Copper (II) Ions from Aqueous Solution Using a Magnetite Nano-Adsorbent from Mill Scale Waste: Synthesis, Characterization, Adsorption and Kinetic Modelling Studies. Nanoscale Research Letters, 2021, 16, 168.	5.7	24
6	Novel PVDF-PVP Hollow Fiber Membrane Augmented with TiO2 Nanoparticles: Preparation, Characterization and Application for Copper Removal from Leachate. Nanomaterials, 2021, 11, 399.	4.1	23
7	Microstructure and superconducting properties of Ca substituted Y(Ba1â^'Ca)2Cu3O7â^'δ ceramics prepared by thermal treatment method. Results in Physics, 2017, 7, 407-412.	4.1	21
8	Effect of PVP as a capping agent in single reaction synthesis of nanocomposite soft/hard ferrite nanoparticles. Journal of Magnetism and Magnetic Materials, 2017, 428, 219-222.	2.3	20
9	Structural, electrical conductivity and dielectric relaxation behavior of LiHf2(PO4)3 ceramic powders. Journal of the Australian Ceramic Society, 2018, 54, 307-316.	1.9	18
10	Electrical conductivity and dielectric studies of MnO 2 doped V 2 O 5. Results in Physics, 2016, 6, 420-427.	4.1	17
11	Contemporary Techniques for Remediating Endocrine-Disrupting Compounds in Various Water Sources: Advances in Treatment Methods and Their Limitations. Polymers, 2021, 13, 3229.	4.5	17
12	An Insight into a Sustainable Removal of Bisphenol A from Aqueous Solution by Novel Palm Kernel Shell Magnetically Induced Biochar: Synthesis, Characterization, Kinetic, and Thermodynamic Studies. Polymers, 2021, 13, 3781.	4.5	17
13	Morphology and dielectric properties of single sample Ni0.5Zn0.5Fe2O4 nanoparticles prepared via mechanical alloying. Journal of Advanced Ceramics, 2014, 3, 306-316.	17.4	16
14	Structural and magnetic properties of yttrium aluminum iron garnet (YAlG) nanoferrite prepared via auto-combustion sol–gel synthesis. Journal of the Australian Ceramic Society, 2018, 54, 55-63.	1.9	16
15	Study the Iron Environments of the Steel Waste Product and its Possible Potential Applications in Ferrites. Advanced Materials Research, 0, 1109, 295-299.	0.3	15
16	Influence of pH Adjustment Parameter for Sol–Gel Modification on Structural, Microstructure, and Magnetic Properties of Nanocrystalline Strontium Ferrite. Nanoscale Research Letters, 2018, 13, 160.	5.7	15
17	Enhancing absorption properties of Mg–Ti substituted barium hexaferrite nanocomposite through the addition of MWCNT. Journal of Materials Science: Materials in Electronics, 2017, 28, 8429-8436.	2.2	13
18	Influence of Pr doping on the thermal, structural and optical properties of novel SLS-ZnO glasses for red phosphor. Results in Physics, 2017, 7, 1202-1206.	4.1	13

#	Article	IF	CITATIONS
19	Magnetic Phase-Transition Dependence on Nano-to-Micron Grain-Size Microstructural Changes of Mechanically Alloyed and Sintered Ni0.6Zn0.4Fe2 O 4. Journal of Superconductivity and Novel Magnetism, 2014, 27, 1451-1462.	1.8	12
20	Influence of indium substitution and microstructure changes on the magnetic properties evolution of Y3Fe5â^'xInxO12 (xÂ=Â0.0–0.4). Journal of Materials Science: Materials in Electronics, 2015, 26, 3596-3609.	2.2	12
21	Complex permittivity and power loss characteristics of α-Fe2O3/polycaprolactone (PCL) nanocomposites: effect of recycled α-Fe2O3 nanofiller. Heliyon, 2020, 6, e05595.	3.2	12
22	Structural and superconducting properties of Y(Ba1-K)2Cu3O7-Î′ ceramics. Ceramics International, 2017, 43, 11339-11344.	4.8	11
23	Influence of aluminum substitution on microstructural, electrical, dielectric, and electromagnetic properties of sol-gel synthesized yttrium iron garnet (YIG). AIP Advances, 2020, 10, .	1.3	11
24	Synthesis of Nano-Magnetite from Industrial Mill Chips for the Application of Boron Removal: Characterization and Adsorption Efficacy. International Journal of Environmental Research and Public Health, 2021, 18, 1400.	2.6	11
25	Effect of Variation Sintering Temperature on Magnetic Permeability and Grain Sizes of Y ₃ Fe ₅ O ₁₂ via Mechanical Alloying Technique. Materials Science Forum, 0, 846, 395-402.	0.3	10
26	Dependence of magnetic and microwave loss on evolving microstructure in yttrium iron garnet. Journal of Materials Science: Materials in Electronics, 2018, 29, 8688-8700.	2.2	10
27	Effect of Ratio in Ammonium Nitrate on the Structural, Microstructural, Magnetic, and AC Conductivity Properties of BaFe12O19. Materials, 2018, 11, 2190.	2.9	10
28	Complex Permittivity and Microwave Absorption Properties of OPEFB Fiber–Polycaprolactone Composites Filled with Recycled Hematite (α-Fe2O3) Nanoparticles. Polymers, 2019, 11, 918.	4.5	10
29	Enhancement of Complex Permittivity and Attenuation Properties of Recycled Hematite (α-Fe2O3) Using Nanoparticles Prepared via Ball Milling Technique. Materials, 2019, 12, 1696.	2.9	10
30	Utilization of Nano-TiO2 as an Influential Additive for Complementing Separation Performance of a Hybrid PVDF-PVP Hollow Fiber: Boron Removal from Leachate. Polymers, 2020, 12, 2511.	4.5	10
31	Preparation and Characterization of Sr _{1â^'x} Nd _x Fe ₁₂ O _{19Derived from Steel-Waste Product via Mechanical Alloying. Materials Science Forum, 0, 846, 403-409.}	;0.3	9
32	Experimental and computational study on epoxy resin reinforced with microâ€sized OPEFB using rectangular waveguide and finite element method. IET Microwaves, Antennas and Propagation, 2020, 14, 752-758.	1.4	9
33	Calcium-Substituted Y3Ba5Cu8O18 Ceramics Synthesized via Thermal Treatment Method: Structural and Superconducting Properties. Journal of Superconductivity and Novel Magnetism, 2019, 32, 1875-1883.	1.8	8
34	Phase, morphological, and magnetic properties of iron oxide nanoparticles extracted from mill scale waste and its surface modification with CTAB surfactant. Journal of the Australian Ceramic Society, 2020, 56, 729-743.	1.9	8
35	Effects of Recycled Fe2O3 Nanofiller on the Structural, Thermal, Mechanical, Dielectric, and Magnetic Properties of PTFE Matrix. Polymers, 2021, 13, 2332.	4.5	8
36	Structural, Electromagnetic and Microwave Properties of Magnetite Extracted from Mill Scale Waste via Conventional Ball Milling and Mechanical Alloying Techniques. Materials, 2021, 14, 7075.	2.9	8

#	Article	IF	CITATIONS
37	Complex Permittivity and Electromagnetic Interference Shielding Effectiveness of OPEFB Fiber-Polylactic Acid Filled with Reduced Graphene Oxide. Materials, 2020, 13, 4602.	2.9	7
38	Magnetite Nanoparticles (MNPs) Used as Cadmium Metal Removal from the Aqueous Solution from Mill Scales Waste Sources. Sains Malaysiana, 2020, 49, 847-858.	0.5	6
39	Extraction of Magnetite from Millscales Waste for Ultrafast Removal of Cadmium Ions. International Journal of Engineering and Advanced Technology, 2019, 9, 5902-5907.	0.3	6
40	Effects of Calcination Temperature on Microstructure and Superconducting Properties of Y123 Ceramic Prepared Using Thermal Treatment Method. Solid State Phenomena, 0, 268, 325-329.	0.3	5
41	Compositional and frequency dependent-magnetic and microwave characteristics of indium substituted yttrium iron garnet. Journal of Materials Science: Materials in Electronics, 2017, 28, 3029-3041.	2.2	5
42	The Effect of MWCNTs Filler on the Absorbing Properties of OPEFB/PLA Composites Using Microstrip Line at Microwave Frequency. Materials, 2020, 13, 4581.	2.9	5
43	Trends of Parallel Microstructure and Magnetic Properties Evolution in Co0.5Zn0.5Fe2O4. Journal of Superconductivity and Novel Magnetism, 2014, 27, 1903-1910.	1.8	4
44	Magnetic Properties and Microstructures of Cobalt Substituted Barium Hexaferrites Derived from Steel Waste Product via Mechanical Alloying Technique. Materials Science Forum, 2016, 846, 388-394.	0.3	4
45	Magnetic phase transition of mechanically alloyed single sample Co0.5Ni0.5Fe2O4. Results in Physics, 2019, 15, 102683.	4.1	4
46	Dielectric behavior of β-SiC nanopowders in air between 30 and 400°C. Journal of Materials Science: Materials in Electronics, 2016, 27, 6623-6629.	2.2	2
47	Electrospun ZnFe2O4/Al: ZnFe2O4 nanofibers for degradation of RhB via visible light photocatalysis and photo-Fenton processes. Journal of Materials Science: Materials in Electronics, 0, , 1.	2.2	2
48	Sintering Temperature Effect on Microstructure and Magnetic Evolution Properties with Nano- and Micrometer Grain Size in Ferrite Polycrystals. , 0, , .		1
49	Dependence of pH Variation on the Structural, Morphological, and Magnetic Properties of Sol-Gel Synthesized Strontium Ferrite Nanoparticles. , 0, , .		1
50	Analysis of thermal and electrical conductivity properties of Al substitution LiHf2(PO4)3 chemical solid electrolyte. SN Applied Sciences, 2019, 1, 1.	2.9	1
51	Experimental and Computational Study of the Microwave Absorption Properties of Recycled <i>α</i> -Fe2O3/OPEFB Fiber/PCL Multi-Layered Composites. Journal of Materials Science and Chemical Engineering, 2022, 10, 30-41.	0.4	1
52	Effect of microstructure on complex permittivity and microwave absorption properties of recycled <i>α</i> -Fe ₂ O ₃ nanopowder prepared by high-energy ball milling technique. Materials Express, 2022, 12, 319-326.	0.5	1
53	Structural transformations of mechanically alloyed polycrystalline YMnO3-based material for gas sensing application. Journal of the Australian Ceramic Society, 2019, 55, 1009-1020.	1.9	0
54	EFFECT OF MILLING TIME ON THE PARTICLES SIZE AND MICROSTRUCTURE OF MILLSCALE DERIVED BaFe ₁₂ O ₁₉ ., 2002, , .		0

#	Article	IF	CITATIONS
55	Removal of Copper Ions from Aqueous Solution Using Waste Mill Scales. Solid State Phenomena, 0, 307, 247-251.	0.3	0